

## Multitemporal Acoustic Backscatter Data Analysis to Monitor the Dynamics of Seabed Surface Sediments

Danar Guruh Pratomo<sup>a,\*</sup>, Khomsin<sup>a</sup>, Irena Hana Hariyanto<sup>a</sup>, Nabilla Aprilia Putri<sup>a</sup>, Imam Mudita<sup>b</sup>,  
Dwi Hariyanto<sup>b</sup>, Ahmad Fawaiz Safi<sup>b</sup>

<sup>a</sup> Department of Geomatics Engineering, Institut Teknologi Sepuluh Nopember, Surabaya 60111, Indonesia

<sup>b</sup> National Research and Innovation Agency (BRIN), Jakarta, 10340, Indonesia

Corresponding author: \*guruh@geodesy.ac.id

**Abstract**—Backscatter strength is a product of underwater acoustic remote sensing. This study used a multibeam echosounder as an acoustic remote sensing instrument to collect backscatter strength data. These data are then used to classify the surficial sediment distribution. To monitor the difference in seabed sediment distribution, a time-series survey was performed to obtain multitemporal acoustic backscatter data. An EM 304 multibeam system from Kongsberg was mounted on the Research Vessel Baruna Jaya III from the Indonesia National Research and Innovation Agency (BRIN). It was used to collect backscatter data in the waters of Raja Ampat, Indonesia. The data were collected at different times, April and July 2021. Geometric and radiometric corrections were applied to these backscatter data. Based on the angular response curve analysis from acoustic backscatter strength, the research area can be classified into four seabed sediment types: boulder, gravel, sand, and mud. A comparison of both time series backscatter data shows that the boulder and gravel areas increased by 13.6% and 19.0%, respectively. Elsewhere, the area with sediment types of sand and mud diminished by 30.5% and 2.0%. The change in the sediment type area occurred as much as 50.5%, while the remaining 49.5% area remained unchanged. This resulting value is apparently derived from the steep topography that rapidly changes sediment distribution. One such suggestion is that sediment sampling should be performed to confirm the model from angular response curve analysis.

**Keywords**—Backscatter strength; multibeam echosounder; multitemporal; sediment classification.

Manuscript received 13 Feb. 2023; revised 7 May 2023; accepted 15 Sep. 2023. Date of publication 31 Dec. 2023.  
IJASEIT is licensed under a Creative Commons Attribution-Share Alike 4.0 International License.



### I. INTRODUCTION

An echosounder is a depth-measuring instrument that uses an acoustic signal to measure the vertical distance between the transducer and the seabed surface. The depth is obtained by calculating the time interval between emitting and returning the acoustic signal and the velocity of the acoustic wave when it propagates through the water column [1]. There are two types of echosounders: single beam and multibeam. The significant difference between these types is the coverage these instruments can collect in one track/transit. A single beam echosounder can only obtain the acoustic response below the transducer as a line, whereas the acoustic response from a multibeam echosounder is collected in a corridor form.

A multibeam echosounder can collect fast and accurate data over a wide coverage area. A multibeam echosounder can be used for underwater acoustic remote sensing in vast scientific applications such as monitoring benthic habitats [2], [3], ocean morphology [4], and sediment formations and

compositions. A multibeam echosounder (MBES) system is the integration of several sensors [5]. The system consists of a depth sensor, a navigation sensor providing time, position, and heading, and an attitude sensor. All these sensors produce data that can compile detailed location information in the research area along with the necessary corrections and calibrations. A MBES records three main data: bathymetry, backscatter, and water column data. The commonly used data from MBES are bathymetric, yet backscatter and water column data have not been used optimally [6].

Backscatter data provide information about the seafloor's acoustic response and distinguish between different types of seafloor sediments, such as hard rock and fine sediment [7]. Another function is to provide information about the characteristics of the seabed environment. These characteristics include seabed hardness, surface sediment characteristics [8], benthic habitat [2], and environmental considerations for managing marine geological resources, including identifying disasters such as seabed landslides.

Backscatter also assists with environmental modeling [9], monitoring of anthropogenic changes in the seabed (e.g., monitoring of pipeline locations) [10], [11], and safety navigation [12] (e.g., monitoring and mapping of rocky areas or areas of hard soil) [13]. The value of the backscatter is based on the proportion of acoustic energy that is reflected from the seabed and produces an impedance contrast. Impedance is the level of ability of an underwater object to transmit (forward or reflect) sound waves that propagate to it. The intensity of the backscatter will later be interpreted as the roughness or hardness of the seabed surface. This value is called backscatter strength (BS) and has decibels (dB) units. Moreover, the orientation of the small-scale seabed topography (the organized seabed roughness) with respect to the navigation direction causes an azimuthal dependence of the BS intensity [14].

The characteristics of seabed sediments are conventionally obtained from the results of coring and grabbing sediment samples. However, this method is slow, expensive, requires a lot of effort, and does not provide real-time or in-situ data collection [15]. Hence, this study uses the backscatter strength value to classify in-situ bottom surface sediment types at the research location in time series or multitemporal. Sediment grain size analysis can provide information about the origin of sediment transport processes within a certain period. The distribution from sediment grain size variations depends on several parameters, such as the distance of the location to the shoreline, the distance from the river/stream, the topography of the area around the watershed, the source of sedimentary material, and the limited sediment transport mechanism in the area. [17], [18]. Sediment transport is defined as the movement of particles due to a combination of gravity acting on the sediment and the movement of fluids causing the movement of the sediment from one place to another [19], [20]. The movement of the sediment depends on the cohesiveness of the sediment type, for example, in the type of boulder and gravel rocks that break down into smaller units or particles due to the physical factors of water and pressure. These particles usually undergo resuspension before finally undergoing transportation and disposition, which takes longer than the type of sand sediment that only undergoes transportation.

Previous research that discussed a similar topic about sediment distribution using MBES has already been studied in various publications, such as a study to analyze the effect of the backscattered signal response which is reflected by bottom sediments using the MBES Kongsberg instrument EM302 [21], [22]. The study results showed that the strength of the backscattering value was between -9 to -67 dB, which was divided into six sediment types, namely mud, sand, gravel, silt, clay, and boulder (rocks). This result was obtained through an analysis using the Angular Response Analysis method. However, this study has a drawback; it did not use validation data to confirm the results. Therefore, the research results were categorized as an estimation. In addition, the difference from the current study lies in the time factor of data acquisition. The current research was conducted in a time series (multitemporal), whereas previous studies only used one acquisition time (one-time factor). Hence, to address these challenges, this current study aims to determine the dynamics of the distribution of bottom surface sediments at

the research site using multitemporal multibeam echosounder data.

## II. MATERIAL AND METHOD

Field data were collected around the Sagawin Strait, West Papua Province, Indonesia, with the coordinates 00°49'01" - 01°00'08" S and 130°28'36" - 131°00'56" E (Fig. 1). This strait lays as a part of the more extensive marine area, Pitt Strait. The Pitt Strait connects Batanta Island and Salawati Island geographically, while in the southwest, there is little Sagawin Island and, connected by Sagawin strait. This Sagawin island is a type of an uninhabited island on the west of Sorong City but administratively part of Raja Ampat Regency [23]. In addition, it is one of the regions of the archipelagic site, Raja Ampat, which is on the tip of the Bird's Head (Vogelkop) Peninsula, see [24], involving the conservation area for endemic faunas, namely kind of fisheries, golden jellyfish, and tropical ave [25], [26], [27]. Based on the morphology of the archipelago, it is estimated that the waters of the Sagawin Strait contain various types of bottom surface sediments.

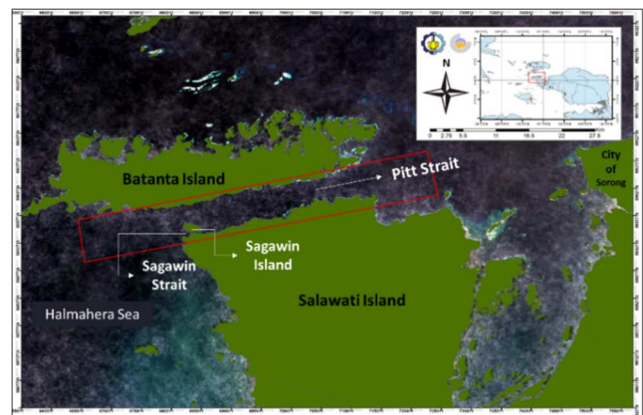


Fig. 1 Current research location

The data was acquired on April 26 and July 18, 2021, using a multibeam echosounder (MBES) EM304 from Kongsberg. MBES Kongsberg EM304 is an MBES with Mill Cross configuration [28] with separate transmitter and receiver components and has a transmit frequency of 26 - 34 kHz. The MBES Kongsberg EM304 sounding depth range can reach 8000m and is equipped with a multibounce dampening technique to reject noise from false echo reflections [29]. This study used a MBES Kongsberg EM304 with 1°x1° beamwidth. This instrument is installed with a gondola on the hull of the Research Vessel (RV) Baruna Jaya III, belonging to the National Research and Innovation Agency (BRIN) [30]. Fig. 2 presents the gondola construction (inset the red line) for MBES installation on RV Baruna Jaya III. The main mission of this vessel is to support mapping and survey activities for marine research and observation.

In this study, the main software used to process the hydrographic survey data was an open-source software named SwathEd. SwathEd is a software program pioneered and developed by the Ocean Mapping Group, University of New Brunswick, Canada [31]. This software has several features and functions that facilitate the processing of bathymetric survey data.



Fig. 2 Gondola mounting Construction on RV Baruna Jaya III

There are many correction data in hydrographic surveys, particularly those using MBES as the main instrument. This condition is substantial considering the MBES function as swath sector acquisition result. Every inch of the data error can represent actual meter features, depending on the instrument installation settings. Hence, the MBES survey and process should run its correction data, including the tidal effect, to determine the vertical datum of each data point and sound velocity profile to estimate the sound velocity, which propagates along the water column. In addition, the attitude or behavior of the acquisition vessel is an essential consideration.

The validation data used in this research are from a sedimentation model managed and published by the Institute of Arctic and Alpine Research (INSTAAR), University of Colorado, Colorado, USA. Corresponding to the fact that this model is integrated from thousands of individual datasets. This convenience still needs to be improved in terms of accuracy and spatial data resolution. Nevertheless, many other researchers are using this model according to the model data reports. The main raw bathymetry data and the correction data are then processed using SwathEd software to perform filtering and cleaning. An MBES Kongsberg EM304 data consists of complex information in one \*.kml data format. Therefore, unraveling the raw data becomes the first step in the process. The raw data should be transformed and mosaicked into raster data to acknowledge the error, gap, and noise. After all of the cleaning and unraveling data process, the initial results are corrected bathymetry data (X, Y, and Z data) and backscatter strength (BS) data (acoustic wave intensity), which imply the seabed surface sediment condition.

To classify the existing seabed surface sediment, the BS data result is then processed using the angular response curve (ARC) method and classified into several sediment categorized. From the previous classification step, all BS data is validated using dbSEABED data from INSTAAR. The data that has successfully passed the minimum standard and sufficiently represents the real seabed condition will be qualified for generating the seabed distribution sediment map. However, unsuccessful data in the validation process should be reprocessed in the backscatter data processing. Because of

the multitemporal acquisition time, the seabed surface sediment classification process is repeated for the whole data. Both bathymetry and backscatter data are overlaid for comparison from one sample location to another.

Most processes in this research are managed in SwathEd, including bathymetric and backscatter data. In the processing step of multibeam echosounder raw data, the recorded depth data will be corrected by the insitu acoustic velocity measurement through Sound Velocity Profile (SVP) data and the actual height of the location to the geoid model using the tides data published by the Geospatial Information Agency (BIG) from periodical observation in the official the tide station near research location, Sorong City., the formula to determine the depth from echosounder data considers the period of each ping (Equation 1), as follows:

$$d = \frac{1}{2} v \cdot \Delta t \quad (1)$$

where  $d$  is depth in meters,  $v$  is the sound velocity in water (m/s), and  $\Delta t$  is the time interval from the time the sound wave is transmitted until it is received by the receiver. In the Digital Terrain Model (DTM) process, a part of main processing, each data point that conceives the X, Y, Z location is then interpolated to generate raster data with a cell resolution of 2.5m.

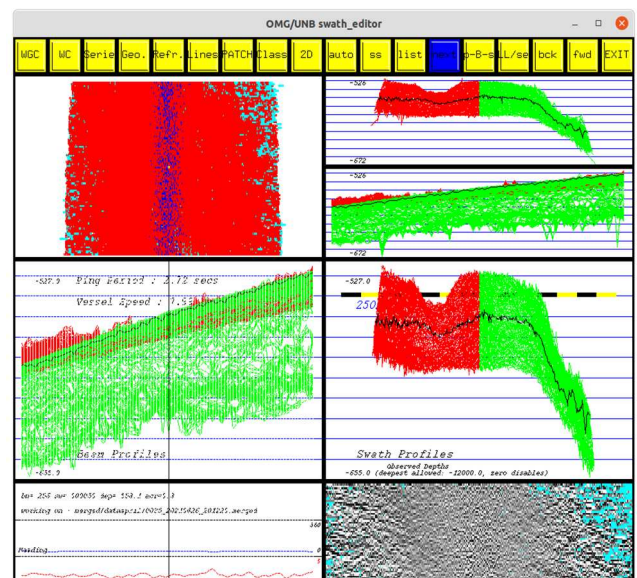


Fig. 3 MBES cleaning process using the SwathEd software

Fig. 3 shows the noise-cleaning process carried out in the Swath Editor window, and this is useful for cleaning data from noise, spikes, or false echoes that are imperfectly reflected. Based on its location, data noise is influenced by certain factors such as ship movement, wave disturbance, and others. The Swath Editor window is divided into several views, namely, the display of amplitude, raw profiles, beam profiles, swath profiles, attitude profiles, and backscatter profiles. The noise-cleaning process is performed on the swath profile display.

Backscatter processing includes correcting the backscatter data on each survey line to the backscatter mosaic process to obtain a complete backscatter strength image at each survey time. Cleaning and filtering are carried out, such as correction

of time-varying gain (TVG) and correction of slant range, until the value of digital number (DN) with 8-bit color graphic is obtained, which is then converted to the value of backscatter strength in each cell through Equation (2) as follows:

$$BS = \frac{DN-255}{2} \quad (2)$$

where  $BS$  is the backscatter strength estimation value, and  $DN$  is the digital number. The process results produce bathymetric data and backscatter data cleaned from noise and gaps. After the mosaicking process, the results show a monochrome color representing the types of seabed surface sediment.

The next challenge is to classify the mosaicking result by using Angular Response Curve (ARC) method. The physical properties of the seabed sediments contribute to the received backscatter value. These properties are related to the bottom water interface (impedance and roughness) and the level of inhomogeneity of the sediment buried in the bottom surface of the water. Each property can contribute more than the other to the strength of the backscatter value depending on the ensonification area. In summary, the ARC method can determine the backscatter value's dependence on the incidence angle. Hereafter, the classification process validation using dbSEABED INSTAAR data is carried out, and the resulting validated sedimentation classification map will be obtained according to the time survey. The first step is to analyze the difference between the two times. The results of overlaying bathymetry data and backscatter strength data are overlaid for April and July 2021.

### III. RESULTS AND DISCUSSION

#### A. Correction Data Result

The sound velocity correction data, SVP, were taken before the depth acquisition was performed using the EM304. Sound speed data is measured on April 10, 2021, at 20.00 UTC for April data. Moreover, sound velocity data was collected for July 18, 2021, at 00:53 UTC. The results show that the minimum and maximum sound wave velocities in April, respectively, were  $1488.81 \text{ ms}^{-1}$  and  $1544.04 \text{ ms}^{-1}$ ; in July, they were  $1483.01 \text{ ms}^{-1}$  and  $1543.36 \text{ ms}^{-1}$ . The tidal correction was also applied to the bathymetric data. The correction is generated based on the tide observations at the Tidal Station from BIG in Sorong. The data has an observation interval of every minute. The same vertical datum is used for both data (April and July 2021): the mean sea level. The tidal data recorded by BIG station in Sorong City belongs to the semi-diurnal type. On April 26, 2021, the lowest tide was 0.71 meters, and the highest was 2.45 meters. Meanwhile, on July 18, 2021, the lowest tide was 1.04 meters, and the highest was 2.09 meters.

#### B. Bathymetry Data Result

Multibeam echosounder raw data may contain bathymetric, water column, and backscatter data. The raw data would then be unraveled in this research to extract the bathymetric and backscatter data. For bathymetric data, generating the raster file format from the point cloud data (raw data) is substantial. Raster data transformation means generating a digital terrain model (DTM) with a spatial resolution of 2.5 m for each pixel—furthermore, cleaning

noise on April 2021 data. There is not much noise in the water column or under the survey data. Neither artifact nor ripple was recorded on the survey data. The most noise found in the April 2021 survey data was at the edge of the survey data.

Meanwhile, for the July 2021 survey, there is considerable noise in the form of ripples and noise at the edges of the survey data in relatively large amounts. The most noise is at the edge of the survey data, resulting from a false echo in the side lobe (beam pattern). The depth data from the survey show that the research location has various primary water morphologies, such as underwater basins and slopes. The depth of the seabed basin is measured from the lowest point to the highest point, as shown in Fig. 4 to Fig.7. The depth of the valley basin in April 2021 data is around 86.988 m, whereas in July 2021, it is around 83.909 m.

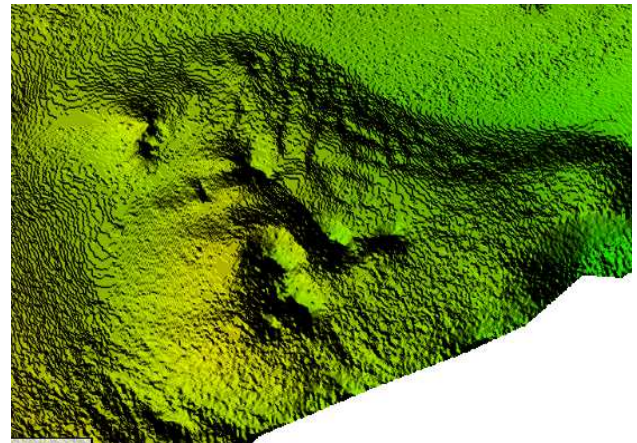


Fig. 4 Underwater basin features in the April Survey: orthogonal view



Fig. 5 Underwater basin features in the April Survey: profile view

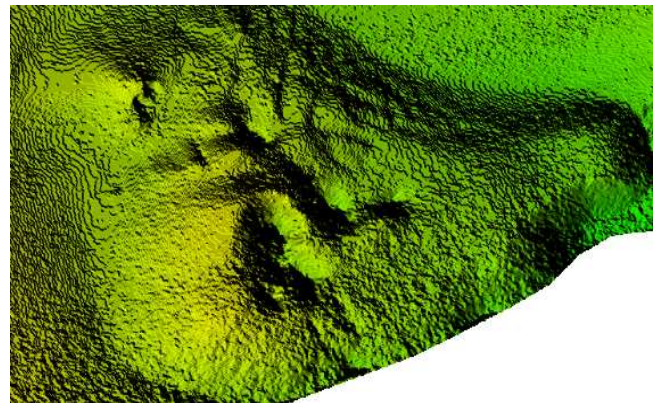


Fig. 6 Underwater basin features in the July Survey: orthogonal view

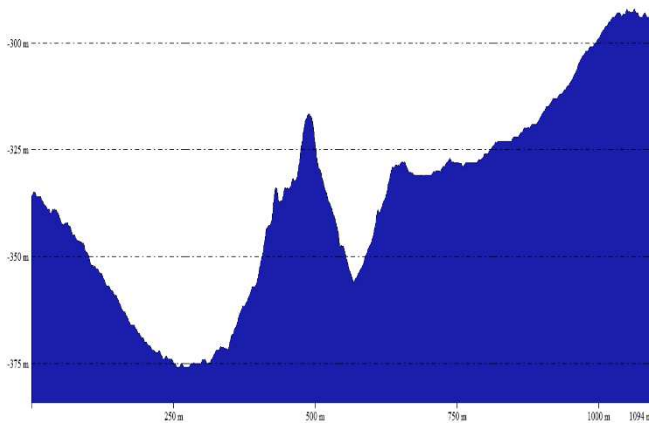


Fig. 7 Underwater basin features in the July Survey: profile view

The difference in depth between April and July can be attributed to the disposition and accumulation of sediment from higher areas to lower basin areas. The seabed slope height (Fig. 8 to Fig. 11) on April survey data is around 107.277 meters. The height of the slopes in the July survey data is about 105.572 meters. Based on these measurements, a difference of approximately 1.705 meters was obtained, which indicates a decrease in the seabed level.

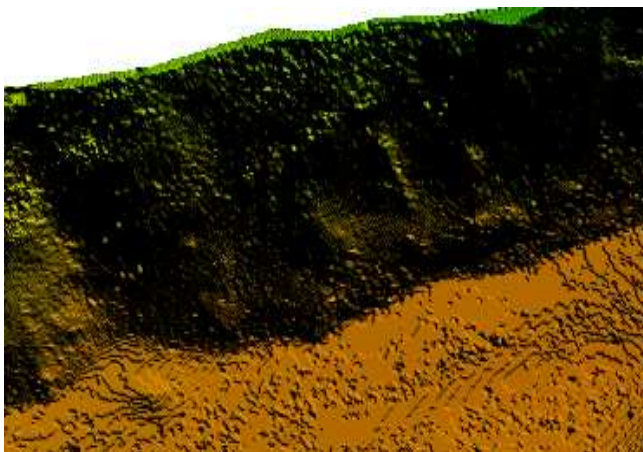


Fig. 8 Slope in the April Survey: orthogonal view

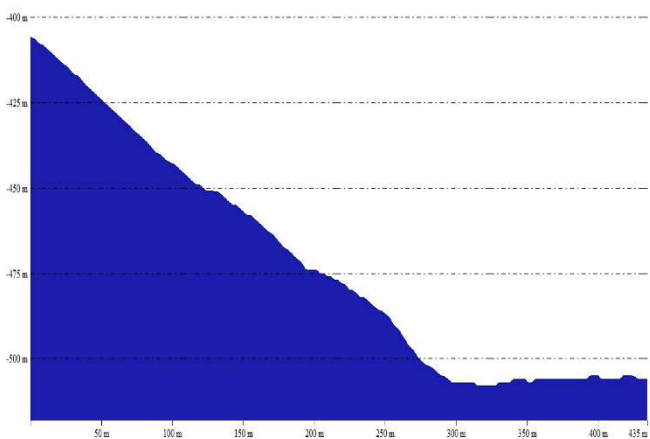


Fig. 9 Slope in the April Survey: profile view

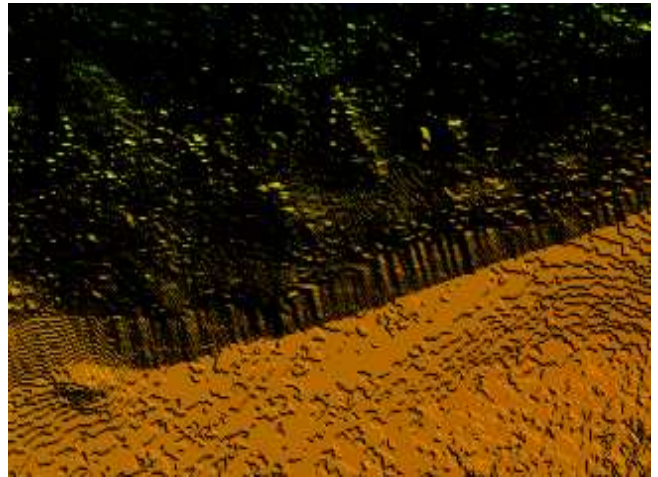


Fig. 10 Slope in the July Survey: orthogonal view

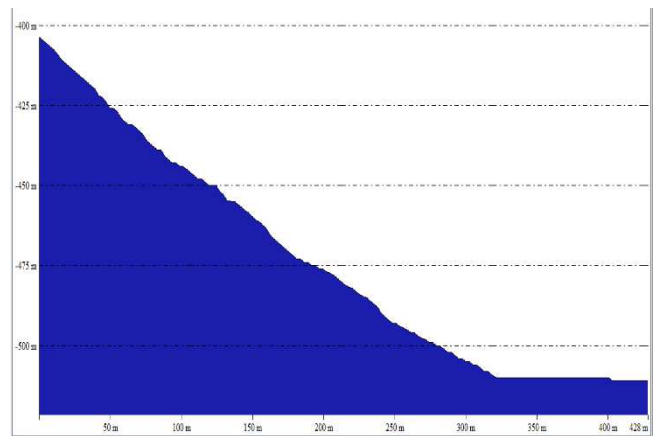


Fig. 11 Slope in the July Survey: profile view

In depth data, the April survey's raw results show depth values with a range of 126 to 702 meters then stretched values out with a new range of 92 to 702 meters. In the visualization, the initial survey or survey data line survey for April 2021 has the deepest depth. This is because the lane's beginning is an area included in the Halmahera Sea area (deep water). The survey results in July showed depth values in the range of 92 meters to 648 meters. As well as the April result, stretching was carried out on the bathymetry value in July with the same range of 92 to 702 meters. The beginning of the survey line visualization represents the most profound depth (Halmahera Sea).

In addition, to estimate the difference between the April and July 2021 bathymetric data, each data point should be calculated through this direct Equation 3, as follows:

$$\Delta h = JB(m) - AB(m) \quad (3)$$

where is the deviation,  $JB$  is the July bathymetric depth result, and  $AB$  is the April bathymetry data. The positive (+) result indicates that the July bathymetry is deeper than the April bathymetry, indicating a decrease in sea level. The deviation results were obtained from three sample sites (Fig. 12) cited effectively in Table I.

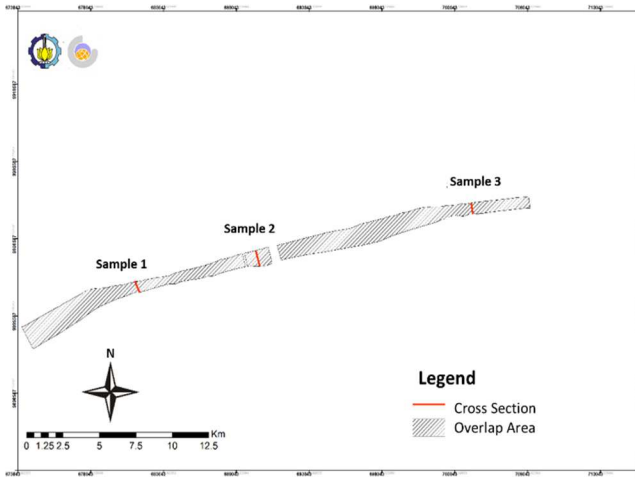


Fig. 12 Bathymetry sample locations

TABLE I

THE AVERAGE OF SHALLOWING AND DEEPENING AT THE SAMPLE POINTS FROM BATHYMETRY DATA DEVIATION RESULTS IN APRIL AND JULY

Sample Point	Shallowing (m)	Subsiding (m)	Dominant
Sample 1	1.768	2.816	Subsiding
Sample 2	3.137	3.983	Subsiding
Sample 3	2.067	2.727	Subsiding

### C. Backscatter Data Result

The mosaic results from the backscatter were analyzed and classified using ArcMap 10.3. The backscatter value mosaicked has a digital number value representing the backscatter strength. The digital number value is then converted to the intensity value in the backscatter value based on Equation 1. The results of the mosaic backscatter value

range from -9 dB to -59 dB for the April mosaic and from 10 dB to -59 dB for the July mosaic. However, this value is equalized from 10 dB to -59 dB to perform comparisons.

Fig. 13 shows each sediment sample location. The classification results from the backscatter values obtained in the April 2021 and July 2021 surveys produced four types of sediment, namely rock (boulder) in the range -9 dB to -22 dB, gravel in the range -23 dB to -34 dB, sand in the range of -35 dB to -48 dB, and mud in the range -49 dB to -59 dB. Table II. represent sediment dynamics over time at three sample points. In sample 1, it is known that there is an increase in the percentage of boulder sediment types by approximately twice the previous area, while the largest decrease occurs in mud sediments with a size of approximately 98.6%.

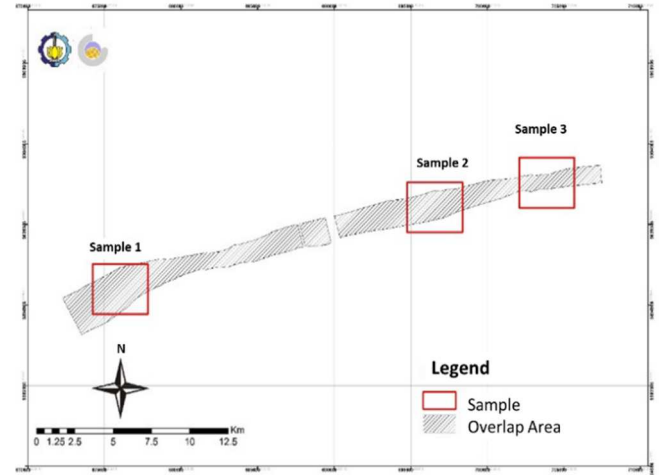


Fig. 13 Sediment sample locations

TABLE II

CLASSIFICATION OF SEDIMENT AT EACH SAMPLE LOCATIONS

Sample	Sediment Type	April, 2021		July, 2021	
		Area (m <sup>2</sup> )	Percentage (%)	Area (m <sup>2</sup> )	Percentage (%)
1	Boulder	21,654.169	0.262	75,045.747	0.908
	Gravel	2,088,883.486	25.274	3,626,660.097	43.880
	Sand	5,449,246.893	65.932	4,553,408.950	55.093
	Mud	705,165.542	8.532	9,835.291	0.119
2	Boulder	25,903.738	0.429	39,489.615	0.654
	Gravel	1,193,021.117	19.758	4,345,306.794	71.964
	Sand	4,809,219.196	79.647	1,645,340.237	27.249
	Mud	10,023.358	0.166	8,030.763	0.133
3	Boulder	321,251.357	8.406	1,187,017.269	31.060
	Gravel	3,324,947.722	87.002	2,562,099.959	67.041
	Sand	165,746.745	4.337	67,835.018	1.775
	Mud	9,745.312	0.255	4,738.897	0.124

According to the area, there was a change in sediment type in 3,011,123.299 m<sup>2</sup> or 36.43% of the total area. In sample 2, there was the largest increase in the amount of sediment, namely in the type of gravel sediment, which was more than twice the amount of the previous sediment. Meanwhile, the type of sediment that experienced the largest decrease was the type of sand sediment, with a percentage decrease of 65.79%. Based on the total area, there was a change in sample 2 with an area of 3,967,494.165 m<sup>2</sup> or 65.71% of the total area. The case in sample 3 shows that only the type of boulder sediment increased with a valuation of more than double the amount of

the previous sediment. The case in sample 3 shows that only the type of boulder sediment increased with a valuation of more than double the amount of the previous sediment. The type of sand sediment experienced the largest amount of shrinkage, namely 59.07%, compared to the previous amount. Based on the area, changes in sediment type in sample 3 occurred in 1,665,899.268 m<sup>2</sup> of the sample area, or 43.59%. Based on the sample results, the overall changes in sediment types in the research area are indicated by the conclusions in Table III and Fig. 14 below.

TABLE III  
DECISIVE SEDIMENT DYNAMICS

Sediment Type	Area on April (m <sup>2</sup> )	Area percentage in April (%)	Area on July (m <sup>2</sup> )	Area percentage in July (%)
Boulder	521,348.917	1.392	5,601,806.219	14.956
Gravel	17,395,777.790	46.443	24,515,585.870	65.452
Sand	18,755,703.220	50.074	7,317,047.283	19.535
Mud	783,021.793	2.091	21,412.344	0.057
<b>Total</b>	<b>37,455,851.720</b>	<b>100</b>	<b>37,455,851.720</b>	<b>100</b>

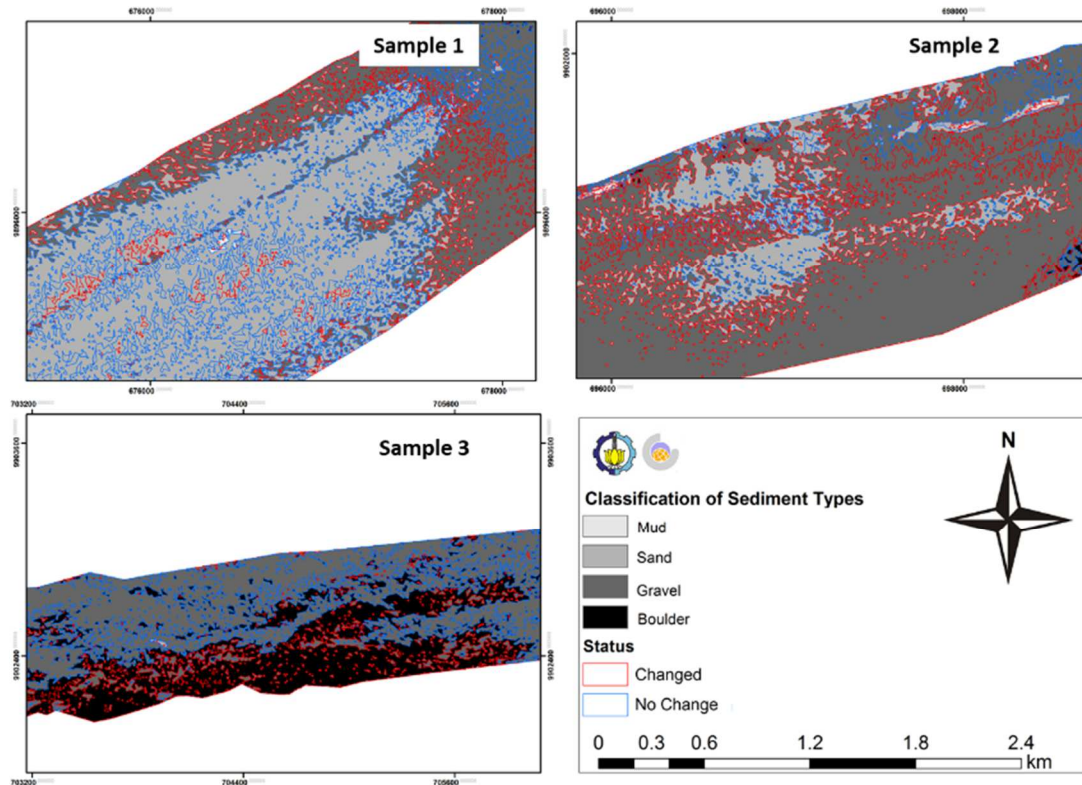


Fig. 14 Decisive sediment dynamics spatially

The study results were then validated with data on types and statistics of seabed lithography from dbSEABED, a maritime database compiled by INSTAAR (The Institute of Arctic and Alpine Research) Colorado University and NOAA. The dbSEABED data comprises a grid with a size of 0.1°. Based on the calculation of the average area, the gravel type has the largest area compared with the other types of sediment, which is around 20.955 km<sup>2</sup>. Sand is the most common type of sediment after gravel, which has an area of approximately 13.036 km<sup>2</sup>. When associated with the dbSEABED data, the composition of most sediments is under the validation data. Despite the positive correlation value between the results and validation data, there are differences in the classification of other sediment types beyond the main results. This is possible because dbSEABED is a database collecting lithology data from third parties, so the details are unclear. However, there are similarities in the species dominance ratio between the dbSEABED data and the research where gravel is the most common type of sediment found in the Sagawin Strait, followed by sand.

#### IV. CONCLUSION

The multibeam echosounder records the survey area's bathymetric, water column, and backscatter data. Through the

extraction process, each data type can be managed appropriately. This study utilized bathymetric and backscatter data from the multibeam echosounder Kongsberg EM304 in multitemporal acquisition, April and July 2021. According to the bathymetric results, the research area has an average depth distribution from 92 to 702 meters concerning the MSL. The survey also recorded various seabed features, such as underwater basins and slopes. Because of the temporal acquisition, the dynamics of the same point can be detected in either shallowing or subsiding. The average difference in bathymetry is about 1.817 meters for the entire bathymetric result. This research focuses on indicating and determining the dynamics of sediment types in the research area using MBES backscatter strength data. Four locations and the survey lanes are used as a sample for validation.

According to the classification of both backscatter strength values, there are four seabed sediment types: boulder (-10 dB to -22 dB), gravel (-23 dB to -34 dB), sand (-35 dB to -48 dB), and mud (-49 dB to -59 dB). Among these sediment types, the dominant sediment in the April survey was sand, and the dominant sediment in July 2021 was gravel. However, the minor type for both time surveys is mud. Several dynamic conditions, adding or subtracting, have been indicated in the research area based on each sediment type. The area of

boulders increased by nearly 13.56%, and also the area of gravel, which is 19.01%.

On the other hand, the sediment types of sand and mud have area losses of 30.54% and 2.03%, respectively. In the aspect of sedimentation, an analysis of changes in sediment type in the study area was obtained. Changes in sediment type occurred as much as 50.48% of the total area, and the remaining 49.52% of the total area did not change. This large change can be triggered by dynamics and seabed phenomena that cause rapid changes in sediment types, such as seabed landslides, which occur due to the steep morphology of the seabed.

#### ACKNOWLEDGMENT

The authors acknowledge the National Research and Innovation Agency (BRIN) for the raw multibeam echosounder data, the Geospatial Information Agency (BIG) for supporting the research by providing the tide data in the surrounding area, and the Institute of Arctic and Alpine Research (INSTAAR) for the best work of integrated seabed surface sediment data. In particular, the authors are grateful for the technical data contribution from the RV Baruna Jaya III crew, who acquired the MBES data. Furthermore, the authors would also like to thank the Ocean Mapping Group (OMG), University of New Brunswick, Canada, as the SwathEd software developer, which is appropriately performed in this work.

#### REFERENCES

- [1] X. Lurton, D. Eleftherakis, and J.-M. Augustin, "Analysis of seafloor backscatter strength dependence on the survey azimuth using multibeam echosounder data," *Marine Geophysical Research*, vol. 39, no. 1–2, pp. 183–203, May 2017, doi: 10.1007/s11001-017-9318-3.
- [2] K. Trzcinska et al., "Spectral features of dual-frequency multibeam echosounder data for benthic habitat mapping," *Marine Geology*, vol. 427, p. 106239, Sep. 2020, doi: 10.1016/j.margeo.2020.106239.
- [3] J. H. Christensen, L. V. Mogenssen, and O. Ravn, "Deep Learning based Segmentation of Fish in Noisy Forward Looking MBES Images," *IFAC-PapersOnLine*, vol. 53, no. 2, pp. 14546–14551, 2020, doi: 10.1016/j.ifacol.2020.12.1459.
- [4] J. Majcher et al., "Using difference modelling and computational fluid dynamics to investigate the evolution of complex, tidally influenced shipwreck sites," *Ocean Engineering*, vol. 246, p. 110625, Feb. 2022, doi: 10.1016/j.oceaneng.2022.110625.
- [5] G. Fromant, N. Le Dantec, Y. Perrot, F. Floch, A. Lebourges-Dhaussy, and C. Delacourt, "Suspended sediment concentration field quantified from a calibrated MultiBeam EchoSounder," *Applied Acoustics*, vol. 180, p. 108107, Sep. 2021, doi: 10.1016/j.apacoust.2021.108107.
- [6] C. Brown, J. Beaudoin, M. Brissette, and V. Gazzola, "Multispectral Multibeam Echo Sounder Backscatter as a Tool for Improved Seafloor Characterization," *Geosciences*, vol. 9, no. 3, p. 126, Mar. 2019, doi: 10.3390/geosciences9030126.
- [7] Putra, F.H. and Pratomo, D.G., *Analisis arus dan transport sediment menggunakan pemodelan hidrodinamika 3 dimension (Studi Kasus: Teluk Ambon, Kota Ambon, Maluku)*. Jurnal Teknik ITS, 2019. 8(2): p. G124-G129.
- [8] Pratomo, D.G. and M.D. Amirullah, *Analisis Data Sub Bottom Profiler Terintegrasi Untuk Identifikasi Sedimen (Studi Kasus: Alur Pelayaran Timur Surabaya)*. Geoid, 2020. 15(1): p. 106-114.
- [9] M. Wang et al., "Using multibeam backscatter strength to analyze the distribution of manganese nodules: A case study of seamounts in the Western Pacific Ocean," *Applied Acoustics*, vol. 173, p. 107729, Feb. 2021, doi: 10.1016/j.apacoust.2020.107729.
- [10] G. Fromant, N. Le Dantec, Y. Perrot, F. Floch, A. Lebourges-Dhaussy, and C. Delacourt, "Suspended sediment concentration field quantified from a calibrated MultiBeam EchoSounder," *Applied Acoustics*, vol. 180, p. 108107, Sep. 2021, doi: 10.1016/j.apacoust.2021.108107.
- [11] Pratomo, D.G., K. Khomsin, and D. Pambudhi, *Deteksi Pipa Bawah Laut Dengan Data Multibeam Echosounder (Studi Kasus: Muara Bekasi)*. Geoid, 2018. 13(2): p. 115-120.
- [12] Pratomo, D.G. and K. Hutanti, *Analisis Pola Sebaran Sedimen Untuk Mendukung Pemeliharaan Kedalaman Perairan Pelabuhan Menggunakan Pemodelan Hidrodinamika 3d (Studi Kasus: Pelabuhan Tanjung Perak, Surabaya)*. Geoid, 2019. 14(2): p. 78-86.
- [13] G. Lamarche and X. Lurton, "Recommendations for improved and coherent acquisition and processing of backscatter data from seafloor-mapping sonars," *Marine Geophysical Research*, vol. 39, no. 1–2, pp. 5–22, May 2017, doi: 10.1007/s11001-017-9315-6.
- [14] T. C. Gaida, T. A. G. P. van Dijk, M. Snellen, T. Vermaas, C. Mesdag, and D. G. Simons, "Monitoring underwater nourishments using multibeam bathymetric and backscatter time series," *Coastal Engineering*, vol. 158, p. 103666, Jun. 2020, doi: 10.1016/j.coastaleng.2020.103666.
- [15] Ayuningtyas, F. and B. Cahyono, *K.K. Jenis dan Sebaran Sedimen Menggunakan Data Multibeam Echosounder Multi-Temporal di Alur Pelayaran Barat dan Timur Surabaya*. JGISE: Journal of Geospatial Information Science and Engineering, 2021. 4(2): p. 140.
- [16] Gemilang, W., et al., *Karakteristik Sebaran Sedimen Pantai Utara Jawa Studi Kasus: Kecamatan Brebes Jawa Tengah*. Jurnal Kelautan Nasional, 2018. 13(2): p. 65-74.
- [17] Abuodha, J., *Grain size distribution and composition of modern dune and beach sediments, Malindi Bay coast, Kenya*. Journal of African Earth Sciences, 2003. 36: p. 41-54.
- [18] Shanshan, W., et al., *Grain size characteristics of surface sediment and its response to the dynamic sedimentary environment in Qiantang Estuary, China*. International Journal of Sediment Research, 2022. 37(4): p. 457-468.
- [19] S. Ouilon, "Why and How Do We Study Sediment Transport? Focus on Coastal Zones and Ongoing Methods," *Water*, vol. 10, no. 4, p. 390, Mar. 2018, doi: 10.3390/w10040390.
- [20] Pratomo, D.G. and M.R.F. Aziz, *Optimasi Penggunaan Sediment Trap Pada Alur Pelayaran Barat Surabaya Menggunakan Pemodelan Transport Sedimen (Studi Kasus: Alur Pelayaran Barat Surabaya, Jawa Timur)*. Geoid, 2020. 15(2): p. 228-239.
- [21] Akbar, K., *Analisis Nilai Hambur Balik Sedimen Permukaan Dasar Perairan Menggunakan Data Multibeam Echosounder EM302*. 2017, Institut Teknologi Sepuluh Nopember: Surabaya.
- [22] Akbar, K., D.G. Pratomo, and K. Khomsin, *Analisis Nilai Hambur Balik Sedimen Permukaan Dasar Perairan Menggunakan Data Multibeam Echosounder EM302*. Jurnal Teknik ITS, 2017. 6(2): p. G152-G155.
- [23] Regency, B.-S.o.R.A., *Raja Ampat Regency in Figures 2021*. 2021, Raja Ampat: BPS-Statistics of Raja Ampat Regency.
- [24] Ali, J.R. and L.R. Heaney, *Wallace's line, Wallacea, and associated divides and areas: history of a tortuous tangle of ideas and labels*. Biological Reviews, 2021. 96(3): p. 922-942.
- [25] C. M. White, S. Mangubhai, L. Rumetna, and C. M. Brooks, "The bridging role of non-governmental organizations in the planning, adoption, and management of the marine protected area network in Raja Ampat, Indonesia," *Marine Policy*, vol. 141, p. 105095, Jul. 2022, doi: 10.1016/j.marpol.2022.105095.
- [26] Edy, S., et al., *A holistic approach to manta ray conservation in the Papuan Bird's Head Seascape: Resounding success, ongoing challenges*. Marine Policy, 2022. 137: p. 104953.
- [27] L. L. Griffiths et al., "Linking historical fishing pressure to biodiversity outcomes to predict spatial variation in Marine Protected Area performance," *Marine Policy*, vol. 139, p. 105024, May 2022, doi: 10.1016/j.marpol.2022.105024.
- [28] F. Mosca et al., "Scientific potential of a new 3D multibeam echosounder in fisheries and ecosystem research," *Fisheries Research*, vol. 178, pp. 130–141, Jun. 2016, doi: 10.1016/j.fishres.2015.10.017.
- [29] Crenan, B. *Kongsberg's EM304 (Installation) and the Result onboard RV Thalassa*. 2018. Woods Hole, Massachusetts: University-National Oceanographic Laboratory System.
- [30] Putra, A., N. Fuad, and T. Handoyo, *Design and finite element analysis of gondola construction for multibeam echosounder (MBES) installation on RV Baruna Jaya III - BPPT*. IOP Conference Series: Earth and Environmental Science, 2022. 972(1): p. 012004.
- [31] Nasby-LucasNM, et al., *Integration of submersible transect data and high-resolution multibeam sonar imagery for habitat-based groundfish assessment of Heceta Bank, Oregon*. 2002.